

The mechanism of the amyloidogenic conversion of T7 endonuclease I

Zhefeng Guo and David Eisenberg*

Howard Hughes Medical Institute, UCLA-DOE Institute for Genomics and Proteomics,
Molecular Biology Institute, UCLA, Box 951570, Los Angeles, CA 90095-1570, USA.

Running Title: Preparation model for the amyloidogenic conversion of T7EI

*Address correspondence to: David Eisenberg, Howard Hughes Medical Institute, UCLA-DOE Institute for Genomics and Proteomics, Molecular Biology Institute, UCLA, Box 951570, Los Angeles, CA 90095-1570, Phone: (310) 825-3754. Fax: (310) 206-3914. E-mail: david@mbi.ucla.edu.

Amyloid fibrils are associated with a range of human disorders. Understanding the conversion of amyloidogenic proteins from their soluble forms to amyloid fibrils is critical for developing effective therapeutics. Previously we showed that T7 endonuclease I forms amyloid-like fibrils. Here we study the mechanism of the amyloidogenic conversion of T7 endonuclease I. We show that T7 endonuclease I forms fibrils at pH 6.8, but not at pH 6.0 or pH 8.0. The amyloidogenicity at pH 6.8 is not correlated with thermodynamic stability, unfolding cooperativity, or solubility. Thermal melting experiments at various pH values show that the protein has a distinctive thermal transition at pH 6.8. The transition at pH 6.8 has a lower transition temperature than the unfolding transitions observed at pH 6.0 and pH 8.0, and leads to a β -rich conformation instead of an unfolded state. Electron microscopy shows that the thermal transition at pH 6.8 results in fibril formation. The thermal transition at pH 6.8 leads to a protein state that is not accessible at pH 6.0 or pH 8.0, showing that the existence of the amyloidogenic conformation of T7 endonuclease I depends sensitively on solution conditions. Therefore, we propose that fibrillizing proteins need to be "prepared" for fibrillization. Preparation may consist of amino acid replacements or changing solution conditions, and may require retention of some aspects of native structure. In this model, some amyloid-enhancing mutations decrease protein stability while others have little effect.

Deposition of amyloid fibrils is associated with a range of human disorders, including Alzheimer's disease, type II diabetes mellitus, and

the transmissible spongiform encephalopathies. For 25 amyloid diseases, specific proteins have been identified as the major fibril component (1). Although amyloid fibrils involved in different diseases share common properties such as fibrillar morphology, affinity to Congo red, and the cross- β X-ray diffraction pattern, their protein components share little similarities in their primary sequences or native structures. An important prerequisite for globular proteins to fibrillize is a conformational change into an amyloidogenic state, a conformation that enables oligomerization and fibrillization through specific intermolecular interactions (2-4). Despite extensive research, the molecular basis of the conformational conversion to the amyloidogenic state is still not fully understood.

Thermodynamic stability has been proposed as a major determinant for the amyloidogenic conversion of globular proteins (5). In fact *in vitro* conversion of proteins to fibrils often requires conditions that destabilize native structures (6-9), and thermodynamic analysis of various mutants associated with familial forms of amyloid diseases shows that these mutations destabilize proteins compared to their wild-type counterparts (10-13), thus lending support for this hypothesis. At the same time, there is also evidence that a substantial fraction of amyloidogenic mutations have little or no effect on protein stability. Studies on prion variants associated with familial forms of prion diseases revealed that some variants have the same stability as the wild-type protein (14,15). Polymorphism at residue 129 of the prion protein, which is known to strongly affect the susceptibility to prion disease, does not correlate with the stability of the prion protein (16). Length of polyglutamine expansion in ataxin-3 associated with spinocerebellar ataxia

type 3 was shown not to affect protein stability (17). Similarly, stability of transthyretin variants associated with familial amyloid polyneuropathies are not always correlated with disease severity (18). These results suggest that destabilization of the native structure is not a general mechanism for the amyloidogenic conversion.

Other protein properties have also been proposed to be the molecular basis of the amyloidogenic conversion. Dumoulin et al. (19) proposed that reduced global cooperativity underlies the amyloidogenicity of lysozyme mutants associated with hereditary systemic lysozyme amyloidosis. Schmittschmitt and Scholtz (20) reported that the pH at which maximal fibril formation of ribonuclease Sa was observed does not correlate with conformational stability, but rather with the pH dependence of protein solubility.

In this work, we study the molecular mechanism of the amyloidogenic conversion of T7 endonuclease I (T7EI)¹, a DNA junction resolving enzyme from bacteriophage T7. T7EI exists naturally as a domain-swapped dimer as shown from its crystal structure (21). Previously we found that T7EI forms fibrils that have amyloid properties including fibrillar morphology, binding to dyes Congo red and thioflavin T, and cross- β diffraction pattern (22). Using protein engineering, we showed that T7EI forms fibrils by a runaway domain swapping mechanism, in which each protein molecule swaps a domain into the complementary domain of the adjacent molecule in the fibril (22). Here we investigate the dependence of fibril formation on solution pH, and compare the stability and thermal melting behavior of T7EI at different pH values. Implications of our findings in terms of the molecular basis of the amyloidogenic conversion are discussed.

EXPERIMENTAL PROCEDURES

Protein expression and purification – The T7EI proteins containing an E65K mutation were expressed and purified as previously described (22), and then buffer exchanged to buffer A (50 mM Na Citrate, pH 6.0, 40 mM NaCl), buffer B (50 mM MOPS, pH 6.8, 40 mM NaCl), or buffer C (50 mM Na Phosphate, pH 8.0, 40 mM NaCl) using 5-mL HisTrap column (Amersham) according to pH requirements. Protein concentration was determined by UV absorption at

280 nm using an extinction coefficient of $24.75 \times 10^3 \text{ M}^{-1} \text{ cm}^{-1}$.

Gel electrophoresis – Gel electrophoresis was performed using PhastSystem (Amersham). For native PAGE, native buffer strips for basic proteins (2% agarose, 4.4% β -alanine, and 4% acetic acid) were prepared, and 4-15% gradient PhastGel was used.

Circular dichroism (CD) spectroscopy – CD spectroscopy was performed on a Jasco J-715 spectrometer equipped with a Jasco PTC-348 temperature controller. For equilibrium unfolding, T7EI proteins in buffers A, B, or C were diluted to 10 μM with the same buffer containing increasing concentrations of guanidine hydrochloride (GdnHCl), and were incubated at room temperature for 30 min. CD signal at 222 nm was recorded at 20°C in a 0.01 cm cell (Starna Cells) by averaging the signal over 30 sec. For thermal melting, the ellipticity was monitored at 222 nm. CD cells with 0.1 cm path lengths (Starna Cells) were used. Temperature was ramped at two degrees per minute with a range of 4–90°C. Protein concentrations were adjusted to 20 μM in buffers A, B, or C. The experiments were done in duplicates. For far-UV wavelength scan, CD cells with 0.01 cm path lengths were used and protein concentrations were adjusted to 85-110 μM in 5 \times diluted buffers A, B, or C. For the CD analysis of T7EI fibrils, T7EI proteins in buffer B were incubated at 37°C for 6 days. Then the fibrils were separated from soluble fractions using a 100-kD cutoff Microcon YM-100 centrifugal filter unit (Millipore) and washed twice with buffer B using the 100-KD cutoff filter. Estimation of protein secondary structure from CD spectra was performed using CDSSTR method with the 43-protein reference set included with CDPro software (23).

Analysis of equilibrium unfolding data – The unfolding data were analyzed with nonlinear least-squares fitting as described in Santoro and Bolen (24) to obtain $\Delta G_{U \rightarrow F}^{H_2O}$, the free energy of unfolding, and the m -value, dependence of the free energy of unfolding in the presence of GdnHCl on the concentrations of GdnHCl.

Electron microscopy (EM) – For EM, fibril samples were applied onto glow discharged 400 mesh copper grids covered with

formvar/carbon film (Ted Pella) and stained with 2% uranyl acetate. Samples were examined under a Hitachi H-7000 electron microscope with an accelerating voltage of 75 kV.

Protein solubility analysis – To determine protein solubility, T7EI solutions were concentrated using a 30 kD cutoff Amicon centrifugal filter unit (Millipore) until visible precipitates were observed. The concentrated protein was filtered through a 100 kD cutoff filter to remove precipitates. Then protein concentration was determined by UV absorption at 280 nm using an extinction coefficient of $24.75 \times 10^3 \text{ M}^{-1} \text{ cm}^{-1}$.

RESULTS

We find that fibril formation of T7EI depends on solution pH. At pH 6.8, T7EI forms aggregates upon incubation at 37°C, as shown by the high-molecular-mass band on native PAGE gel (Fig. 1). EM reveals that these aggregates are composed of protein fibrils (Fig. 2b). We have previously shown that these fibrils have amyloid-like properties such as binding to Congo red and thioflavin T, and a cross- β X-ray diffraction pattern (22). At pH 6.0 or 8.0, however, T7EI remains soluble after incubation at 37°C for 3 days, as judged by native gel electrophoresis (Fig. 1). No fibrils were observed when the samples at pH 6.0 and pH 8.0 were viewed under electron microscope (Fig. 2a, c). However, we observe some amorphous aggregates for the samples of pH 6.0 and pH 8.0 (Fig. 2a, c). These aggregates probably formed during sample preparation for EM because of high protein concentration (6 mg/mL).

In order to check whether or not the different behavior of T7EI at different pH values is due to the effect of pH on thermodynamic stability, equilibrium unfolding experiments with GdnHCl as a chemical denaturant were performed. The unfolding of T7EI in the presence of GdnHCl is >95% reversible judged from the recovery of the CD spectrum (data not shown). Under all three pH conditions, the unfolding of T7EI is best characterized by a two-state transition, without any detectable intermediates (Fig. 3). Thermodynamic parameters of unfolding were obtained by fitting the unfolding data to a two-state model (see Experimental Procedures) and the

results are listed in Table 1. We find that T7EI is most stable at pH 8.0, and least stable at pH 6.0, so the amyloidogenicity of T7EI does not correlate with thermodynamic stability. Cooperativity of unfolding, represented by the m -value, does not correlate with amyloidogenicity either, as the m -value of T7EI at pH 6.8 is higher than that at pH 6.0, but lower than that at pH 8.0. We also find that T7EI is most soluble at pH 6.0, and least soluble at pH 8.0, with solubility of $771 \pm 4 \mu\text{M}$, $594 \pm 6 \mu\text{M}$, and $309 \pm 5 \mu\text{M}$ at pH 6.0, 6.8, and 8.0, respectively. Thus, correlation is absent between any of protein stability, cooperativity of unfolding, or solubility and amyloidogenicity of T7EI.

To further investigate the nature of pH effect, thermal denaturation monitored by CD was performed at different pH values. We find that T7EI is denatured at pH 6.0 and pH 8.0 with a transition region that starts at $\sim 55^\circ\text{C}$ (Fig. 4a, c). The denaturation of T7EI at pH 6.0 and pH 8.0 is irreversible, as evidenced by visible precipitates in the CD cell and loss of CD signal when temperature is decreased below the transition region. The mean residue ellipticity at 222 nm ($[\theta]_{222\text{nm}}$) of T7EI changes from about $-7000 \text{ deg cm}^2 \text{ dmol}^{-1}$ to about $-1000 \text{ deg cm}^2 \text{ dmol}^{-1}$ upon denaturation at both pH 6.0 and pH 8.0, indicating loss of secondary structure. The melting curve at pH 6.8 has characteristics that are different from those at pH 6.0 or 8.0 (Fig. 4b). Although thermal melting at pH 6.8 also leads to irreversible changes of CD signal, there are no visible aggregates in the CD cell, suggesting that thermal melting at pH 6.8 leads to soluble oligomers. Thermal melting at pH 6.8 changes $[\theta]_{222\text{nm}}$ from about $-7000 \text{ deg cm}^2 \text{ dmol}^{-1}$ to about $-5000 \text{ deg cm}^2 \text{ dmol}^{-1}$, suggesting that most of the secondary structure remains intact. The transition region at pH 6.8 starts at $\sim 45^\circ\text{C}$, 10°C lower than that at pH 6.0 or 8.0, suggesting that the transition at pH 6.8 requires smaller free energy change than the transition at pH 6.0 or 8.0. Further studies with far-UV CD show that thermal denaturation at pH 6.0 or 8.0 is accompanied by nearly completely loss of CD signal because of precipitation of the protein (Fig. 5a, c), while thermal transition at pH 6.8 leads to a conformation that is characterized by the existence of significant amount of secondary structure (Fig. 5b). Computational analysis of the

secondary structure from far-UV CD spectra shows that, at pH 6.8, thermal transition leads to a β -rich conformation (Fig. 5b, inset). Far-UV CD analysis of the T7EI fibrils show that its CD spectrum is very similar to the CD spectrum of T7EI at 80°C at pH 6.8, consistent with the idea that the 45°C transition at pH 6.8 is an amyloidogenic transition (Fig. 6).

In order to further investigate whether or not the thermal transition at pH 6.8 leads to an amyloidogenic conformation, we examined T7EI by EM at different pH values when incubated at 80°C. Incubation of T7EI samples (20 μ M) at pH 6.0 or 8.0 for 10 min results in the appearance of amorphous aggregates (Fig. 7a, b), consistent with the CD results (Fig. 5a, c). Incubation of T7EI samples at pH 6.8 at 80°C for 1-5 min leads to formation of globular oligomers, and incubation for 10 min results in formation of fibrils (Fig. 7c). These results show that the thermal transition at pH 6.8 is indeed an amyloidogenic transition.

DISCUSSION

The amyloidogenic conversion of T7EI does not correlate with thermodynamic stability, unfolding cooperativity, or solubility.

We find that T7EI forms amyloid-like fibrils at pH 6.8, but changing the solution pH to 6.0 or 8.0 abolishes fibril formation, as judged by gel electrophoresis (Fig. 1) and EM (Fig. 2). Our finding of a dependence of fibril formation on solution pH provides an opportunity to study the molecular basis of fibrillization by comparing the intrinsic properties of T7EI at different pH values. Previous studies had suggested that the property of adopting an amyloidogenic conformation may be determined by thermodynamic stability (10-13), unfolding cooperativity (19), or protein solubility (20). We find that the amyloidogenicity of T7EI does not correlate with any of these, suggesting that these properties by themselves cannot account for the amyloidogenic conversion of T7EI from a native conformation to an amyloidogenic conformation (Fig. 3 and Table 1). Our results are consistent with the findings of several other studies that amyloidogenicity cannot be attributed simply to thermodynamic stability (14-18). Other protein properties must be considered in order to

understand the molecular basis of the amyloidogenic conversion.

Thermal melting of T7EI reveals an amyloidogenic transition at pH 6.8, but not at pH 6.0 or 8.0.

In order to investigate the basis of the amyloidogenicity of T7EI at pH 6.8, we studied the thermal melting of T7EI at three pH values. To our surprise, we find that T7EI shows a thermal transition at pH 6.8 distinctly different from those at pH 6.0 and pH 8.0. At pH 6.0 and pH 8.0, T7EI displays a normal thermal denaturation curve as monitored by CD. As the temperature increases to \sim 55°C, the CD signal changes abruptly, characteristic of a transition region in which protein cooperatively unfolds to a denatured state (Fig. 4a, c and Fig 5a, c). Thermal transition at pH 6.8, however, differs from those at pH 6.0 and pH 8.0 in a number of ways. The thermal transition region at pH 6.8 starts around 45°C, 10°C lower than that at pH 6.0 or 8.0 (Fig. 4b). More importantly, the thermal transition at pH 6.8 does not lead to a denatured state as seen at pH 6.0 or 8.0. Instead, a β -rich conformation is observed following the thermal transition at pH 6.8 (Fig. 5b). This β -rich conformation is similar to the conformation of T7EI fibrils formed by incubation at 37°C, as shown by the CD spectrum of T7EI fibrils (Fig. 6). The CD spectrum of this β -rich conformation also shares characteristics with the amyloidogenic intermediates of at least 11 other proteins (2) including SH3 domain (6), α -synuclein (25), and A β (26). The CD spectra of these amyloidogenic intermediates all have an ellipticity of around -10,000 deg cm² dmol⁻¹ at 200 nm and an ellipticity of about -5000 deg cm² dmol⁻¹ near 222 nm (2). Our EM studies confirmed that the thermal transition at pH 6.8 is an amyloidogenic transition that leads to fibrillization (Fig. 7c).

What is the structural basis of the amyloidogenic transition at pH 6.8? Studies of a T7EI double-cysteine mutant show that T7EI forms fibrils via a runaway domain swapping mechanism, in which each protein molecule swaps a domain into the complementary domain of the adjacent molecule in the fibril (22). The fibril formation of T7EI requires opening of the domain-swapped dimer to form an open-ended dimer, and

the open-ended dimer can form higher order oligomers readily. Therefore, we postulate that, as depicted in Fig. 8, the amyloidogenic transition at pH 6.8 corresponds to the formation of the open-ended dimer, while the thermal transition at pH 6.0 or 8.0 is a denaturation step. The formation of open-ended dimer requires disruption of only one of the two domain-swapped dimer interfaces, so the energy change for this transition would be smaller than that of complete unfolding. This feature is consistent with the observation that the transition at pH 6.8 starts at $\sim 10^\circ\text{C}$ lower than the transition at pH 6.0 or 8.0 (Fig. 4). In addition, the formation of open-ended dimer would not completely disrupt the secondary structure of the protein, consistent with the result of far-UV CD measurement (Fig. 5b).

Examination of the crystal structure of T7EI suggests that the pH dependence of fibrillization may be due to the interaction between His 85 of one subunit and Pro 42' of the other subunit in the domain-swapped dimer (Fig. 9). Because the fibril formation of T7EI is modulated by pH in a range of 6.0 to 8.0, residues that are sensitive to pH changes in this range are presumably histidines. T7EI protein contains four histidines at positions 50, 78, 85, and 116. Histidines 50, 78, and 116 are involved in intramolecular interactions, but His 85 interacts with Pro 42' of the other subunit in the domain-swapped dimer. The H85-P42' interaction stabilizes the domain-swapped dimer, and thus prevents the formation of the open-ended dimer. Therefore, changing solution pH could change H85-P42' interaction and subsequently fibril formation. The involvement of His 85 in the pH dependent domain swapping could be tested by measuring the pKa of His 85 by NMR. It is possible that other residues also contribute to this transition. The full atomic details of the pH dependence of fibrillization require further investigation.

The amyloidogenic transition at pH 6.8 may not result solely from pH effects. We used citrate, MOPS, and phosphate for buffers at pH 6.0, 6.8, and 8.0, respectively (see Experimental Procedures), it is possible that these buffers interact with the protein and contribute to the amyloidogenic conversion or the absence of amyloidogenic conversion. It is known that

different ions could have dramatic effects on protein folding and stability, a phenomenon known as Hofmeister ion effects (27). However, our results show that the amyloidogenic conversion at pH 6.8 does not correlate with protein solubility and stability, which are often indicators of Hofmeister ion effects, suggesting that Hofmeister ion effects may play a limited role in the amyloidogenic conversion at pH 6.8. A complete understanding of the amyloidogenic conversion at pH 6.8 would require an investigation of all possible factors that affect a protein's folding, stability, and conformational changes.

Implications for the molecular basis of the amyloidogenic conversion.

The mechanism of the amyloidogenic conversion of globular proteins has been largely attributed to destabilization of the native structure (5-13). One assumption underlying the protein stability hypothesis is that the amyloidogenic state exists in a protein's conformational ensemble and is in equilibrium with the native state. Therefore, destabilization of the native structure would increase the population of the amyloidogenic conformer. Once the concentration of the amyloidogenic conformer exceeds some critical concentration, stable fibril seeds form and fibrillization occurs (28). Supporting evidence for this hypothesis includes that *in vitro* fibril formation usually requires partially denaturing conditions and that mutations associated with familial forms of amyloid diseases often decrease protein stability (6-13). This hypothesis, however, cannot explain those amyloid-enhancing mutations that do not decrease protein stability (14-18). Such an example is the present work, in which we show that the amyloidogenicity of T7EI at pH 6.8 does not correlate with protein stability (Table 1).

In order to explain the amyloidogenic conversion of T7EI, we present a "preparation" model as illustrated in Fig. 10. We propose that a protein's conformational ensemble is modulated by protein sequence and solution conditions, and the amyloidogenic state exists only in certain conformational ensembles. We refer to the protein conformational ensemble containing the amyloidogenic conformer as the "prepared" ensemble, and the one without the amyloidogenic conformer as the unprepared ensemble. Only

proteins of a prepared ensemble can form amyloid fibrils, and once a protein is prepared, destabilization becomes the primary mechanism for fibrillization. The key point of the preparation model is the existence of a protein conformational ensemble that does not contain the amyloidogenic conformer. In the case of T7EI, at pH 6.8, the thermal melting curve shows a 45°C transition that leads to the accumulation of amyloidogenic conformers and fibril formation (Fig. 4b, and 7c). At pH 6.0 and pH 8.0, the thermal melting experiments show that the 45°C transition does not exist and only a 55°C transition leading to amorphous aggregation is observed, suggesting that the amyloidogenic conformer does not exist under these conditions (Fig. 4a, c and 7a, b). We conclude that the inability of T7EI to form fibrils at pH 6.0 and pH 8.0 results from the absence of the amyloidogenic conformer. We also show that, for a prepared conformational ensemble, destabilization of the native structure facilitates fibril formation. At pH 6.8, it takes three days for T7EI to form fibrils at 37°C (Fig. 1 and 2), but it takes only 10 minutes for T7EI to form fibrils at 80°C (Fig. 7c). Therefore, the preparation model complements the protein stability hypothesis by providing additional explanations for the effects of amino acid replacements and solution conditions on amyloid fibril formation.

The preparation model is consistent with a large body of experimental data. This model can explain why some amyloid-enhancing mutations do not decrease protein stability (14-18). In this case, the mutations prepare the protein for amyloid formation by making the amyloidogenic state accessible without affecting protein stability. Mutations could affect the folding kinetics and the formation of various intermediate states of a nascent polypeptide chain, and thus determine the accumulation of aggregation prone conformers. In addition, fibril formation *in vitro* often requires specific solution conditions, not just any partially denaturing conditions. For example, it was shown that complete or partial unfolding of human muscle acylphosphatase is not by itself sufficient for fibril formation in the absence of

trifluoroethanol (29). Fibrillization of β 2-microglobulin *in vitro* was shown to be critically dependent on the pH and the ionic strength of the solution (30). Requirement of specific solution conditions suggests that the amyloidogenic conformation exists only in these conditions, consistent with the preparation model.

At structural level, the preparation model suggests that the amyloidogenic conversion requires specific conformational changes rather than general unfolding. General unfolding only changes the population of various conformers in the conformational ensemble towards the high-energy state without creating new conformers. If the amyloidogenic conformer did not exist in the protein conformational ensemble, fibrillization wouldn't occur by simply changing the relative energy level of various conformers. Specific conformational changes may include retention of some native structures as several studies suggest that amyloid formation can start from native-like state (17,31-34). In the case of domain-swapped proteins such as T7EI, the dimer interface has to be preserved in order to take advantage of native interactions. We postulate that similar native-like interactions may also be preserved in other systems where fibrillization starts from native-like structures. For example, it was shown that fibril formation of β 2-microglobulin is controlled by the cis-trans isomerization of Pro 32 (35,36), and the fibrillization can be catalyzed by binding to Cu^{2+} (35). Fibrillization of the chicken α -spectrin SH3 domain requires a specific single mutation in the protein sequence (37). These findings support the idea that specific conformational changes and native-like interactions are important for amyloid fibril formation.

Acknowledgements – We thank David M. J. Lilley at University of Dundee, UK for providing the clone of T7EI E65K mutant, Martin Phillips at UCLA DOE-Biochemistry Instrumentation Facility for assistance, and NSF and HHMI for support.

REFERENCES

1. Westermark, P. (2005) *FEBS J.* **272**, 5942-5949
2. Uversky, V. N., and Fink, A. L. (2004) *Biochim. Biophys. Acta* **1698**, 131-153

3. Rochet, J. C., and Lansbury, P. T. (2000) *Curr. Opin. Struct. Biol.* **10**, 60-68
4. Kelly, J. W. (1998) *Curr. Opin. Struct. Biol.* **8**, 101-106
5. Cohen, F. E., Pan, K. M., Huang, Z., Baldwin, M., Fletterick, R. J., and Prusiner, S. B. (1994) *Science* **264**, 530-531
6. Guijarro, J. I., Sunde, M., Jones, J. A., Campbell, I. D., and Dobson, C. M. (1998) *Proc. Natl. Acad. Sci. USA* **95**, 4224-4228
7. Khurana, R., Gillespie, J. R., Talapatra, A., Minert, L. J., Ionescu-Zanetti, C., Millett, I., and Fink, A. L. (2001) *Biochemistry* **40**, 3525-3535
8. McParland, V. J., Kalverda, A. P., Homans, S. W., and Radford, S. E. (2002) *Nat. Struct. Biol.* **9**, 326-331
9. Chiti, F., Taddei, N., Bucciantini, M., White, P., Ramponi, G., and Dobson, C. M. (2000) *EMBO J.* **19**, 1441-1449
10. Hurler, M. R., Helms, L. R., Li, L., Chan, W. N., and Wetzel, R. (1994) *Proc. Natl. Acad. Sci. USA* **91**, 5446-5450
11. Abrahamson, M., and Grubb, A. (1994) *Proc. Natl. Acad. Sci. USA* **91**, 1416-1420
12. Kim, Y. S., Wall, J. S., Meyer, J., Murphy, C., Randolph, T. W., Manning, M. C., Solomon, A., and Carpenter, J. F. (2000) *J. Biol. Chem.* **275**, 1570-1574
13. Ramírez-Alvarado, M., Merkel, J. S., and Regan, L. (2000) *Proc. Natl. Acad. Sci. USA* **97**, 8979-8984
14. Liemann, S., and Glockshuber, R. (1999) *Biochemistry* **38**, 3258-3267
15. Swietnicki, W., Petersen, R. B., Gambetti, P., and Surewicz, W. K. (1998) *J. Biol. Chem.* **273**, 31048-31052
16. Hosszu, L. L., Jackson, G. S., Trevitt, C. R., Jones, S., Batchelor, M., Bhelt, D., Prodromidou, K., Clarke, A. R., Waltho, J. P., and Collinge, J. (2004) *J. Biol. Chem.* **279**, 28515-28521
17. Chow, M. K. M., Ellisdon, A. M., Cabrita, L. D., and Bottomley, S. P. (2004) *J. Biol. Chem.* **279**, 47643-47651
18. Hammarström, P., Jiang, X., Hurshman, A. R., Powers, E. T., and Kelly, J. W. (2002) *Proc. Natl. Acad. Sci. USA* **99**, 16427-16432
19. Dumoulin, M., Canet, D., Last, A. M., Pardon, E., Archer, D. B., Muyldermans, S., Wyns, L., Matagne, A., Robinson, C. V., Redfield, C., and Dobson, C. M. (2005) *J. Mol. Biol.* **346**, 773-788
20. Schmittschmitt, J. P., and Scholtz, J. M. (2003) *Protein Sci.* **12**, 2374-2378
21. Hadden, J. M., Convery, M. A., Declais, A. C., Lilley, D. M. J., and Phillips, S. E. V. (2001) *Nat. Struct. Biol.* **8**, 62-67
22. Guo, Z., and Eisenberg, D. (2006) *Proc. Natl. Acad. Sci. USA* **103**, 8042-8047
23. Sreerama, N., and Woody, R. W. (2000) *Anal. Biochem.* **287**, 252-260
24. Santoro, M. M., and Bolen, D. W. (1988) *Biochemistry* **27**, 8063-8068
25. Uversky, V. N., Li, J., and Fink, A. L. (2001) *J. Biol. Chem.* **276**, 10737-10744
26. Kirkitadze, M. D., Condrón, M. M., and Teplow, D. B. (2001) *J. Mol. Biol.* **312**, 1103-1119
27. Baldwin, R. L. (1996) *Biophys. J.* **71**, 2056-2063
28. Harper, J. D., and Lansbury, P. T., Jr. (1997) *Annu. Rev. Biochem.* **66**, 385-407
29. Calamai, M., Chiti, F., and Dobson, C. M. (2005) *Biophys. J.* **89**, 4201-4210
30. McParland, V. J., Kad, N. M., Kalverda, A. P., Brown, A., Kirwin-Jones, P., Hunter, M. G., Sunde, M., and Radford, S. E. (2000) *Biochemistry* **39**, 8735-8746
31. Plakoutsi, G., Bemporad, F., Calamai, M., Taddei, N., Dobson, C. M., and Chiti, F. (2005) *J. Mol. Biol.* **351**, 910-922
32. Pedersen, J. S., Christensen, G., and Otzen, D. E. (2004) *J. Mol. Biol.* **341**, 575-588
33. Soldi, G., Bemporad, F., Torrassa, S., Relini, A., Ramazzotti, M., Taddei, N., and Chiti, F. (2005) *Biophys. J.* **89**, 4234-4244
34. Eakin, C. M., Attenello, F. J., Morgan, C. J., and Miranker, A. D. (2004) *Biochemistry* **43**, 7808-7815
35. Eakin, C. M., Berman, A. J., and Miranker, A. D. (2006) *Nat. Struct. Mol. Biol.* **13**, 202-208

36. Jahn, T. R., Parker, M. J., Homans, S. W., and Radford, S. E. (2006) *Nat. Struct. Mol. Biol.* **13**, 195-201
37. Morel, B., Casares, S., and Conejero-Lara, F. (2006) *J. Mol. Biol.* **356**, 453-468

FOOTNOTES

¹The abbreviations used are: T7EI, T7 endonuclease I; GdnHCl, guanidine hydrochloride; CD, circular dichroism; EM, electron microscopy.

FIGURE LEGENDS

Figure 1. The native PAGE gel of T7EI at three pH values and two temperatures defines the conditions for fibril formation. T7EI at a concentration of 300 μ M in buffers at three pH values was incubated at 4°C or 37°C for 3 days, and then was run on a native PAGE gel. Fibrils (indicated by arrows) were trapped in the stacking gel and at the boundary of stacking gel and running gel only for protein at pH 6.8 at 37°C.

Figure 2. Electron micrographs of T7EI incubated at 37°C for 3 days. (a) pH 6.0. (b) pH 6.8. (c) pH 8.0. Notice that fibrillar aggregates are found at pH 6.8 but not at pH 6.0 or 8.0.

Figure 3. Equilibrium unfolding of T7EI using GdnHCl as denaturant. The solid lines are the results of nonlinear least-squares fits to a two-state unfolding model. (a) pH 6.0. (b) pH 6.8. (c) pH 8.0. The fit shows (see Table 1) that T7EI has intermediate stability at pH 6.8.

Figure 4. Thermal melting of T7EI at three pH values monitored by CD. (a) pH 6.0. (b) pH 6.8. (c) pH 8.0. Notice that the thermal transition at pH 6.8 starts at lower temperature than those at pH 6.0 or 8.0. At pH 6.8, T7EI initially remains soluble and retains β structure (see text).

Figure 5. Far-UV CD spectra of T7EI at three pH values and two temperatures. (a) pH 6.0. (b) pH 6.8. (c) pH 8.0. The inset table shows the percentage of α and β structures estimated using the CDSSTR method (see Experimental Procedures). Notice that T7EI at pH 6.8 retains β structure even at 80°C.

Figure 6. Far-UV CD spectrum of T7EI fibrils. Notice that this spectrum resembles that of T7EI incubated at pH 6.8 at 80°C (reproduced here for comparison, dotted trace), suggesting that T7EI at these conditions is an oligomeric, amyloidogenic structure.

Figure 7. Electron micrographs of T7EI samples incubated at 80°C. (a, b) T7EI at pH 6.0 (a) and pH 8.0 (b) incubated at 80°C for 10 min. (c) T7EI at pH 6.8 incubated at 80°C for 1-10 min. Scale bars: 100 nm. Notice that incubation of T7EI at 80°C at pH 6.0 and pH 8.0 leads to amorphous aggregates. Incubation of T7EI at pH 6.8 first results in formation of globular oligomers within 5 min, then fibrils at 10 min.

Figure 8. Schematic summary of the outcome of thermal transitions of T7EI at various pH values. Only at pH 6.8 does heating lead to amyloidogenesis.

Figure 9. Ribbon diagram of T7EI with His 85 and Pro 42' shown in stick models. The coordinates are taken from molecules A and B of PDB file 1FZR (21). Notice that the intermolecular H85-P42' interaction may prevent the opening of the domain-swapped dimer.

Figure 10. A model for "Preparation" in which a protein's conformational ensemble is modulated by changing solution conditions or amino acid replacements, permitting access to the amyloidogenic state. N, native state; I, intermediate state on the folding/unfolding pathway, which may not exist for all proteins; U, unfolded state; A, amyloidogenic state; F, fibrillar state.

TABLES

Table 1. Changes in the free energies of unfolding of T7EI. Notice that at the amyloidogenic pH of 6.8, the native protein is intermediate in both stability ($\Delta G_{U \rightarrow F}^{H_2O}$) and cooperativity of unfolding (m -value).

	$\Delta G_{U \rightarrow F}^{H_2O}$ (kcal mol ⁻¹)	m -value (kcal mol ⁻¹ M ⁻¹)
pH 6.0	5.3 ± 0.5	4.9 ± 0.4
pH 6.8	5.9 ± 0.5	6.2 ± 0.5
pH 8.0	7.5 ± 0.6	7.0 ± 0.5

$\Delta G_{U \rightarrow F}^{H_2O}$, free energy of unfolding in the absence of GdnHCl.

m -value, dependence of $\Delta G_{U \rightarrow F}$ on the concentration of GdnHCl.

Figure 1

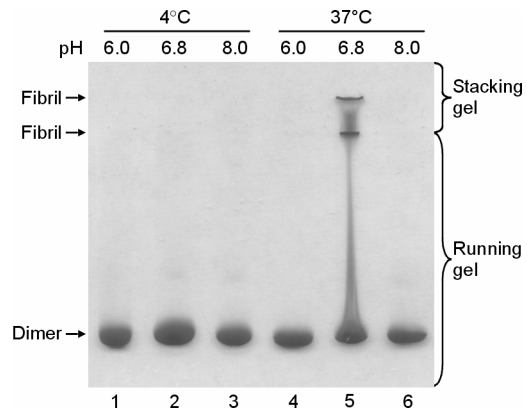


Figure 2

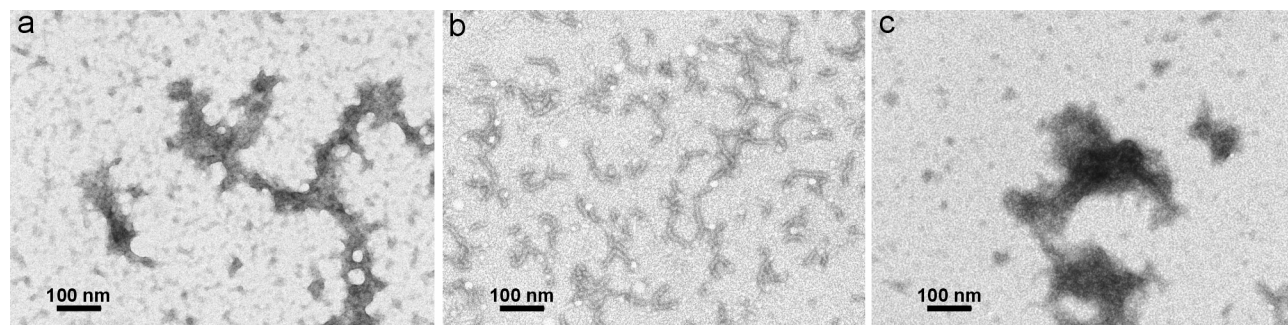


Figure 3

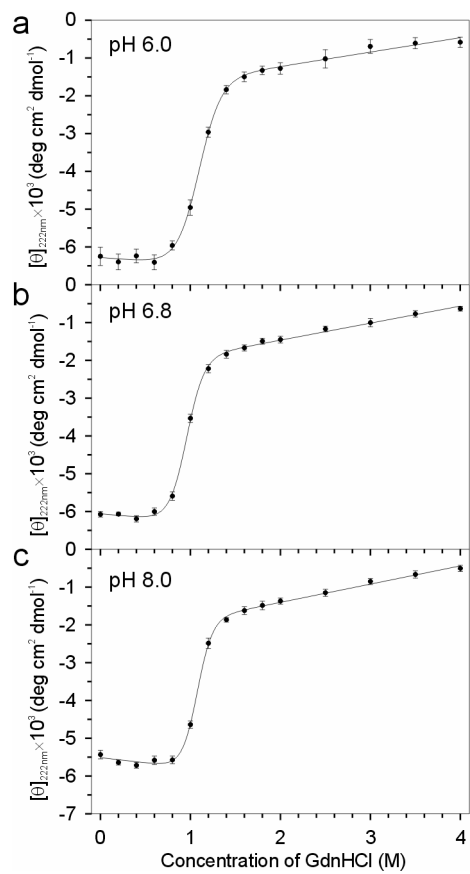


Figure 4

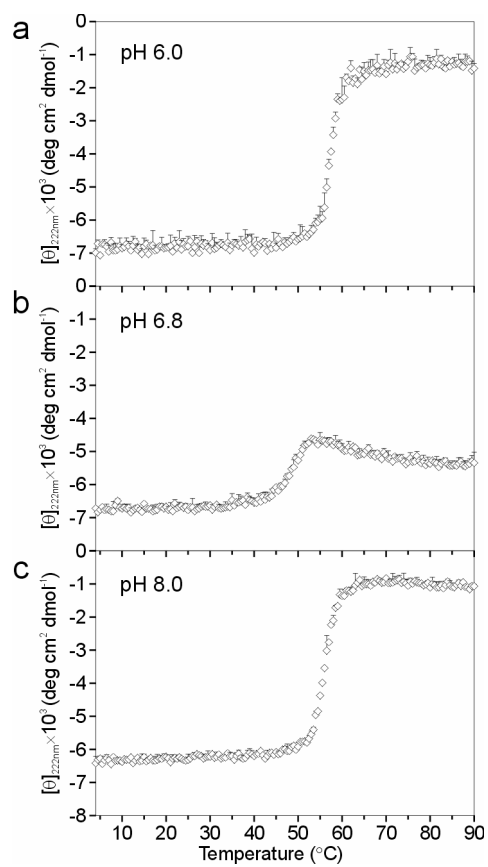


Figure 5

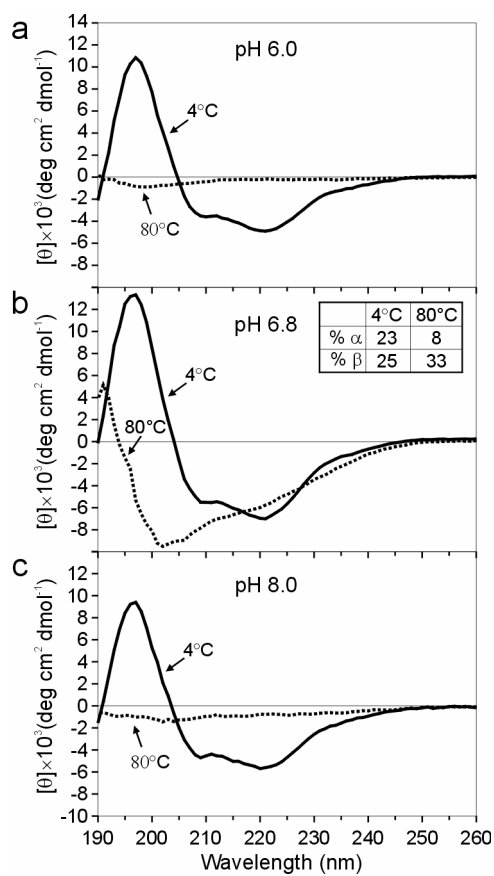


Figure 6

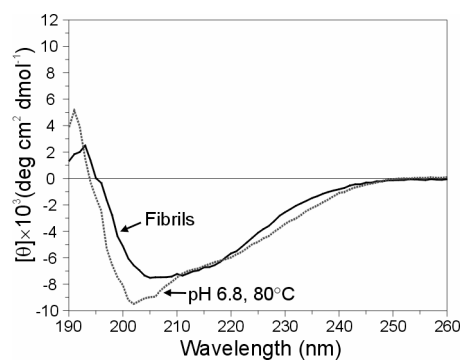


Figure 7

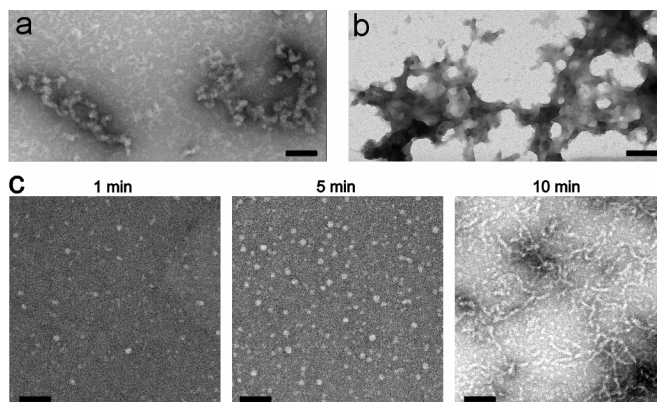


Figure 8

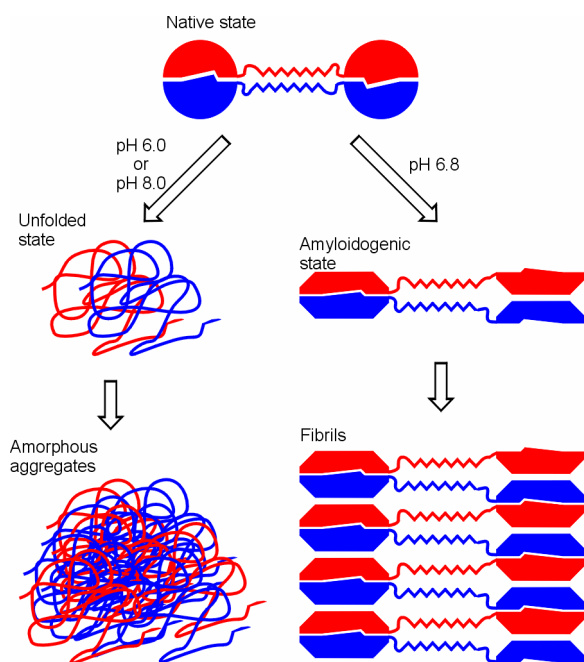


Figure 9

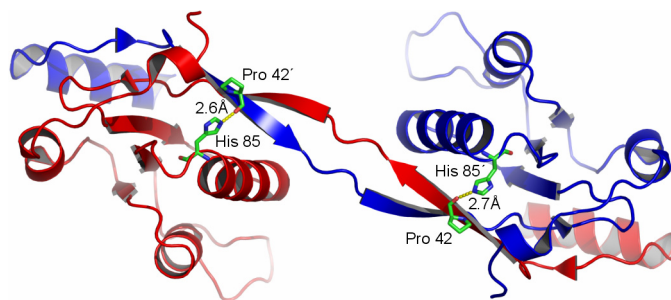


Figure 10

